

Selection of thermal, spectroscopic, spectrometric, and chromatographic methods for characterizing historical celluloid

Christina Elsässer^{1,2}  | Anna Micheluz¹  | Marisa Pamplona¹  |
Stefani Kavda¹  | Peter Montag³ 

¹Conservation Science Department, Deutsches Museum, Munich, Germany

²Chair of Non-destructive Testing, Technical University of Munich, Munich, Germany

³Analytical Service Department, PSS, Polymer Standards Service GmbH, Mainz, Germany

Correspondence

Christina Elsässer, Conservation Science Department, Deutsches Museum, Museumsinsel 1, 80538 Munich, Germany.
Email: c.elsaesser@deutsches-museum.de

Abstract

Celluloid in museum collections is very unstable; therefore, heritage professionals carry out research studies dedicated to understanding its decay and prolonging its lifetime. This paper addresses the need to compare and select suitable analytical methods for that purpose. Thermogravimetric analysis coupled with Fourier transform infrared spectroscopy, evolved gas analysis–mass spectrometry, double shot – gas chromatography/mass spectrometry, and gel permeation chromatography (GPC) were employed to characterize the emission of gasses (decay products) and measure the molecular weight and camphor (plasticizer) content from unaged, artificially, and naturally aged celluloid samples. A pioneer GPC set-up for the quantification of camphor was introduced for the first time in this study. Results demonstrated that GPC was the most suitable method for assessing material changes due to degradation. Both set-ups, for measuring molecular weight and quantifying camphor, appear promising for assessing the effect of conservation treatments and investigating the heterogeneous degradation of celluloid objects in future studies.

KEYWORDS

degradation, plasticizer, separation techniques, spectroscopy, thermogravimetric analysis

1 | INTRODUCTION

Cellulose nitrate (CN) is considered a milestone in the history of polymers since it marked the starting point for the commercial use of plastics by the end of the 19th century.¹ Thanks to its versatile properties, such as good processability and the ability to faithfully imitate natural materials, CN products with a luxurious and precious appearance were affordable to a broad public.² Countless CN objects of daily use, such as combs, toys, eyeglass frames, instrumental keys, technical instrument dials,

jewelry, collars, and photographic films, are nowadays preserved in many historical museum collections.^{3–8} Renowned constructivist artists of the 20th century, namely Naum Gabo, Antoine Pevsner, and László Moholy-Nagy, also used CN for their artworks.^{9–12}

It has been well documented that CN is one of the most unstable plastics.^{3,7} The increased rate of degradation and the fact that it is autocatalytic, renders its preservation particularly challenging. The chemical and physical degradation of CN involves the following processes:

This is an open access article under the terms of the Creative Commons Attribution License, which permits use, distribution and reproduction in any medium, provided the original work is properly cited.

© 2021 The Authors. *Journal of Applied Polymer Science* published by Wiley Periodicals LLC.

1. Hydrolysis of nitro groups. It is one of the most significant degradation processes, leading to the emission of nitrous gases.^{8,12,13} In combination with moisture in the air, these gases form nitric acid, which accelerates the polymer decomposition and catalyzes the degradation of other artifacts in proximity.
2. Chain scission. The CN polymer chain length, indicated by the Molecular weight (M_w), is reduced mainly due to chemical and physical degradation.^{8,12,14} For unaged commercial celluloid products the M_w ranges between 20,000 and 312,000 Da.^{15–16}
3. Loss of plasticizer. This is another important degradation process and takes place through migration, evaporation, or sublimation. The terpenoid camphor was the most commonly used plasticizer in CN, forming a product known as celluloid.^{4,5,7} Although camphor was costly and not easily accessible, and other plasticizers have been used as its substitutes (e.g. triphenylphosphate and diethyl- or dibutyl phthalates), camphor remained the standard plasticizer for CN.^{7,17–20} It is normally present in considerable amounts (20–33% wt/wt).^{6,7,15,20} Several authors have also detected camphor in combination with other plasticizers, such as glycerol triacetate, several phthalates, triphenylphosphate and n-ethyl acetanilide.^{10,12}

Due to the instability of celluloid in museum collections, several research projects worldwide are meeting the challenge to prolong the lifetime of this material by exploring effective and sustainable storage conditions,^{21–23} absorbents and packaging systems.²⁴

Such research projects use analytical methods to characterize celluloid decay products and assess material changes associated with the three aforementioned, main degradation processes. However, the authors are not aware of any published systematic study aiming at selecting the most suitable analytical methods for that purpose. In this paper, a multi-analytical approach is employed to study the effects of the chemical and physical degradation of celluloid, particularly with thermogravimetric analysis coupled with Fourier transform infrared spectroscopy (TGA-FTIR), evolved gas analysis–mass spectrometry (EGA-MS), double shot – gas chromatography/mass spectrometry (TD/Py-GC/MS), and gel permeation chromatography (GPC).

TGA has been previously employed in the field of conservation science to study the percentage weight-loss of gaseous products from cellulose esters.^{14,25–27} However, when employed with the simultaneous identification of the evolved gases of nitrocellulose, which the hyphenated technique TGA-FTIR can provide, studies focused on highly-nitrated (nitrogen >12%) energetic material (that is dynamites and gun propellants).^{28–30} Given that museum

collections mostly comprise low-nitrated (nitrogen <12%) objects plasticized with camphor, which have been rarely examined, this study employs TGA-FTIR to understand their thermal decomposition.

EGA-MS and TD/Py-GC/MS are powerful techniques developed from analytical pyrolysis.³¹ The use of EGA-MS and Py-GC/MS, without the addition of TD (thermal desorption), in the context of cultural heritage has increased in recent years, with studies concerning the degradation of organic materials, including plastic artifacts, and identification of their gaseous products.^{31–35} Among them, only a few have investigated celluloid objects; Schilling et al.³⁶ have characterized celluloid from the SamCo reference collection with EGA-MS, in the context of the POPART project³⁷, while Sutherland et al.¹⁰ have investigated a cellulose ester artwork by Naum Gabo with Py-GC/MS. No studies however were encountered in the literature to have coupled Py with TD in the same technique, TD/Py-GC/MS, to study celluloid.

GPC, also known as size exclusion chromatography, is a powerful technique for characterizing the molecular weight distribution (MWD) of polymers.^{38–39} It has been mainly used for the study of native, unmodified cellulose,^{40–41} cellulose in the form of pulp^{42–43} or fibers⁴⁴ and highly-nitrated cellulose used in the past in explosives.^{45–48} Only a few studies have employed GPC to investigate degradation in low-nitrated celluloid objects in museum and cultural heritage collections.^{8,12} In this study, in addition to the use of GPC for characterizing the MWD, a new GPC-method is introduced, which enables to quantification of the amount of camphor.

All the techniques employed here are very demanding and laborious, costly to acquire and maintain, and require a high level of expertise. Therefore, this study addresses the research community in the field of heritage science and hopes to contribute to it by presenting the most suitable analytical techniques for assessing the effects of conservation treatments and artificial aging experiments on celluloid.

1.1 | Research aims

This paper, first and foremost, aims to evaluate TGA-FTIR, EGA-MS, TD/Py-GC/MS, and GPC for their suitability to characterize celluloid decay products and assess material changes associated with hydrolysis of nitro groups, loss of plasticizer and chain scission. For this purpose, unaged as well as artificially and naturally aged celluloid samples were used.

Secondly, this paper aims to showcase the potential of technique(s) evaluated as the most suitable, by characterizing the heterogeneous nature of degraded celluloid on areas of samples that macroscopically show different levels of degradation.

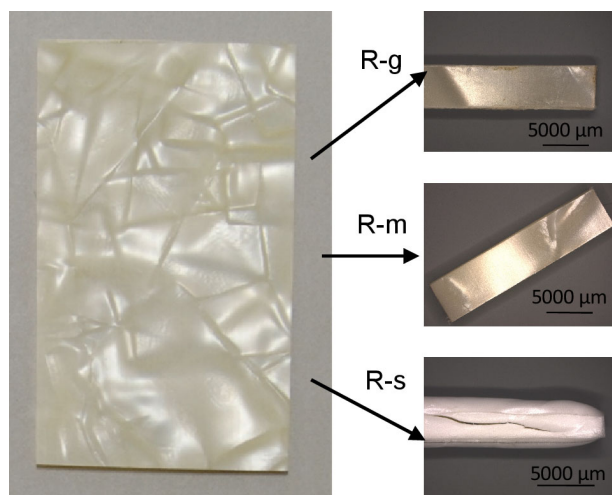


FIGURE 1 A celluloid plate imitating mother of pearl cut into stripes (dimension: $20 \times 5 \times 1.5 \text{ mm}^3$) before and after artificial aging. R-g: Reference sample in good condition; R-m: Reference sample in moderate condition; R-s: Reference sample in severe condition [Color figure can be viewed at wileyonlinelibrary.com]

2 | EXPERIMENTAL

2.1 | Materials

2.1.1 | Artificially aged celluloid for evaluation of analytical techniques

New celluloid plates, which are nowadays used as inlays for musical instruments, imitating beige-colored mother of pearl (Cream Large Pattern Pearloid Celluloid Sheet IN640, $200 \times 100 \times 1.5 \text{ mm}^3$) were purchased from Rothko and Frost™. Three replicates (R-g) were kept as unaged reference material to represent surfaces in good condition without signs of degradation (Figure 1). A number of samples were thermally aged according to the following methods simulating moderate and severe aging conditions, respectively:

- R-m: reference material ($n = 3$) in moderate condition, without visual changes. The samples were placed in a fan-assisted dynamic climate chamber MKF 115 (Binder) at 70°C with varying relative humidity (RH) levels between 10% (for 1 h) and 98% (for 1 h) for 100 cycles (in total around 300 h).
- R-s: reference material ($n = 3$) in severe condition, with deformation, discoloration and cracking. The samples were placed in a 1 L glass desiccator in an oven (VL 115, VWR™) maintained at 70°C for 28 days. To gain a saturated RH a glass test tube filled with de-ionized water was enclosed in the desiccator along with the samples.

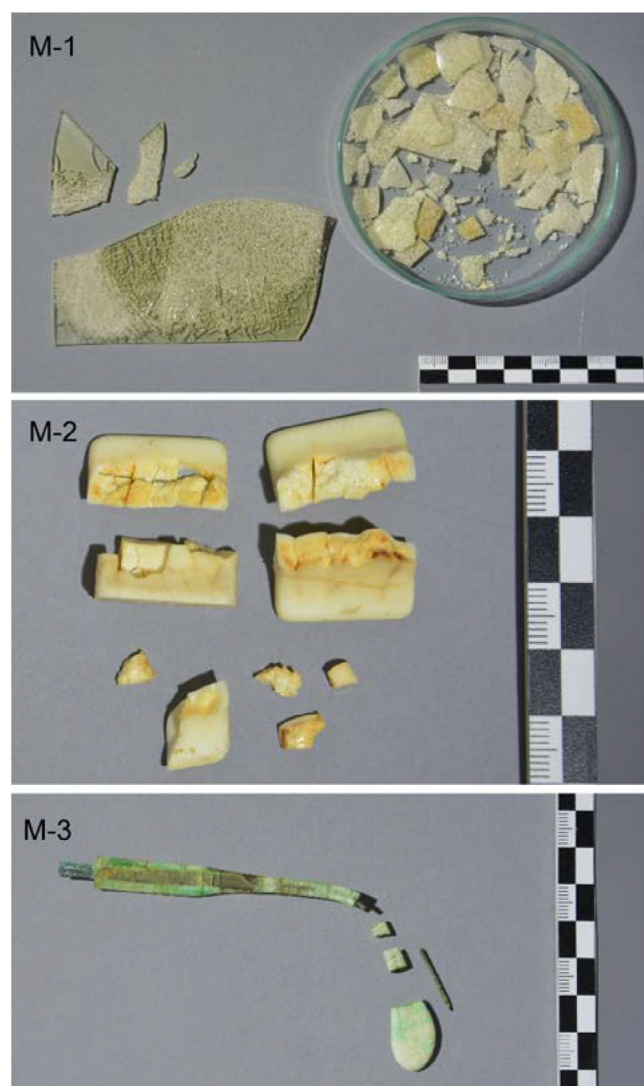


FIGURE 2 Naturally aged celluloid museum objects in severe condition: M-1: Transparent plate; M-2: Beige musical keys; M-3: Transparent spectacle frame [Color figure can be viewed at wileyonlinelibrary.com]

After thermal aging, the samples were stored during the measurements at room temperature in a safety storage cabinet (Q90.195.120, asecos®) with permanent filtered (active charcoal) air ventilation, and were kept in the dark to prevent degradation by light.

2.1.2 | Naturally aged museum celluloid for evaluation of analytical techniques

All investigated naturally aged objects were in a very poor condition (Figure 2) and were therefore deaccessioned from the collection and/or donated to the Conservation Science Department of the Deutsches

Museum for research purposes. The museum objects were thus extensively sampled:

- M-1: Transparent plate of unknown date from the former company Hutmacher & Schlund (Switzerland). In 2007 C. Heiner found these transparent plates in sealed boxes in the storage area of the company and acquired them for his private collection. In 2017 C. Heiner donated several plates for this study. The former transparent plate has turned yellow, embrittled throughout, severely cracked, crazed and fallen apart in many pieces.
- M-2: Beige musical keys belonged to a technical instrument (Hohnerola) for the electronic sound generation of the Siemens-studio dated from 1956. The Hohnerola can be seen at the permanent exhibition of musical instruments at the Deutsches Museum. As the off-gassing keys were corroding the metal parts of the instrument and seriously harming the object, they were removed and stored separately. The keys are very fragile, crumbling and with internal cracks.
- M-3: Transparent spectacle frame. The production date is unknown, but its form and shape resemble designs of the 1950s/1960s. Until its deaccession, it belonged to the Deutsches Museum optics collection. The frame has cracked, crazed and turned greenish due to corrosion of the internal metal part.

2.1.3 | Artificially aged celluloid for describing the heterogeneous nature of degraded celluloid

A transparent colorless plate (Incudo Clear Transparent Celluloid Sheet RF0425, $430 \times 290 \times 0.5 \text{ mm}^3$) was

obtained from Rothko and Frost™. Three replicates (P-g) were kept as unaged reference material to represent surfaces in good condition. Samples were cut as coupons ($40 \times 40 \text{ mm}^2$) to be thermally aged at 70°C and 75% RH in a fan-assisted dynamic climate chamber (MKF 115, Binder) for 32 days. A hole was drilled in one of their corners from which samples were mounted on a glass rod to allow air circulation around them during aging.

The transparent colorless plate (0.5 mm) displays two distinct areas after thermal aging (Figure 3):

- P-u: the lower half of the sample visually appears physically undamaged (no cracks, crazes, embrittlement).
- P-d: the upper half shows physical damages such as internal stresses and crazing. At the points where many crazes have formed, air bubbles are visible.

2.1.4 | Naturally aged museum celluloid for describing the heterogeneous nature of degraded celluloid

For information about this material see above description for M-1 (sec. 2.1.2). Sampling was undertaken from two distinct areas of this material (Figure 3):

- M1-n: Samples from very few areas that are still transparent, but have yellowed, and show no cracking or crazing.
- M1-d: Damples from areas that have lost their transparency, severely cracked, crazed, and embrittled.

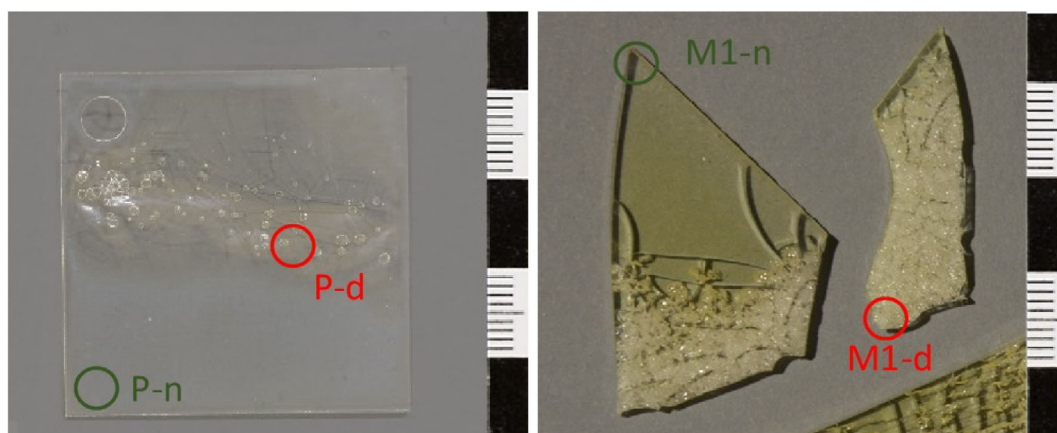


FIGURE 3 Selected samples to showcase the heterogeneous nature of degraded celluloid: Artificially aged transparent colorless plate (P) (left) and piece of the naturally aged transparent plate M-1 (right). The green circles indicate the sample positions, which macroscopically appear without physical damage (P-n and M1-n), while the red circles specify the sample positions, which macroscopically appear physically damaged, cracked or crazed (P-d and M1-d) [Color figure can be viewed at wileyonlinelibrary.com]

3 | METHODS

3.1 | Thermogravimetric analysis coupled with infrared spectroscopy

Non-isothermal thermogravimetry was applied to study the thermal stability of samples in triplicate. A TGA-system TG 209 F1 Libra (Netzsch) was employed to monitor mass changes of the samples during the heating program. Around 10 mg of sample was placed in an open 85 μl alumina crucible and heated from room temperature, at a rate of $10^\circ\text{C}/\text{min}$, to 550°C under a flow of nitrogen (20 ml/min purge gas and protective gas flow rate). The volatiles released during the thermal degradation were detected by a coupled Bruker Alpha FTIR spectrometer. To prevent the condensation of volatile compounds, the balance adapter, transfer tube and FTIR gas cell were maintained at 200°C . All spectra were continuously recorded in the spectral range of $4000\text{--}600\text{ cm}^{-1}$ with 16 scans at a spectral resolution of 4 cm^{-1} . Proteus Thermal Analysis (Netzsch) software and OPUS 8.1 (Bruker) software with EPA_NIST.S01 database were used for TGA curve interpretation and compound identification, respectively.

For the integration of intensity of nitrous oxide (N_2O) and nitric oxide (NO), the absorption bands of N_2O at 2238 cm^{-1} and NO at 1907 cm^{-1} , which did not overlap with signals of other functional groups, were selected. Bands were baseline corrected and calculated using OPUS 8.1 (Bruker) software. The quantification of the correspondent volatiles considered the absorption area between 2264 and 2224 cm^{-1} for N_2O and between 1980 and 1880 cm^{-1} for NO.

3.2 | Evolved gas analysis–Mass spectrometry

The evolution of gas production arising from heated samples was detected using a Multi shot Pyrolyzer EGA/PY-3030D (Frontier Lab.). Around 200 μg of sample was added directly into a stainless-steel Eco-cup sample holder (Frontier Lab.). The temperature program was between 100 and 700°C (for 5 min) at a ramp of $20^\circ\text{C}/\text{min}$. Evolved gas was transferred directly into the 5977B MSD mass spectrometer (Agilent) through a deactivated and uncoated stainless-steel transfer Frontier Ultra Alloy® EGA tube (UADTM 2.5 N-2.5 m-I.D. 0.15 mm, O.D. 0.47 mm, Frontier Lab.) maintained at 300°C into the 7890B GC system oven (Agilent). Analyses were performed with Helium as carrier gas at a flow rate of $1.2\text{ ml}/\text{min}$ and a split ratio 25:1. Ion detection was carried out in the m/z range 25–550. The thermogram

interpretations and volatile identifications were performed by means of EGA-curve comparison and selective m/z extraction with the F-Search 3.5.0 (Frontier Lab.) software and database.

3.3 | Double shot–Gas chromatography/mass spectrometry

In order to collect more information about the volatile and polymeric decay products, double-shot-GCMS (see instrument details in sec. 3.2) was employed on 100 μg sample. The first step, thermal desorption (TD-GC/MS), was carried out from 50°C (for 2 min) to 220°C (for 3 min) with an increasing ratio of $20^\circ\text{C}/\text{min}$ and cryo-trap at -180°C for the volatile focalization. This was followed by the second step, flash pyrolysis (Py-GC/MS), at 600°C (for 6 s). GC separations were performed using a Frontier UA5 capillary column (30 m-0.25F, $30\text{ m} \times 250\text{ }\mu\text{m} \times 0.25\text{ }\mu\text{m}$, Frontier Lab.), the carrier gas Helium with a flow rate of $1.2\text{ ml}/\text{min}$ and a split ratio of 30:1. The injector temperature was set at 300°C . The column temperature program was: 40°C for 2 min, $20^\circ\text{C}/\text{min}$ to 280°C for 5 min. The MS parameters were: electron impact (EI) at 70 eV in positive mode, source temperature at 230°C , transfer line at 280°C , quadrupole temperature at 150°C and scanning mass range of 15–550 m/z . An MSD Mass Hunter Workstation Ver. B.0700 SP2 (Agilent Technologies) software was used for data analysis, while the EI mass spectra of compounds were compared to NIST MS Search 2.2 and F-Search 3.5.0 (Frontier Lab.) databases.

3.4 | Gel permeation chromatography

Two different instrumental set-ups were applied for: (1) detecting the average M_w of CN polymer and (2) quantifying camphor.

For (1) ca. 3 mg of sample was dissolved in 1 ml of N,N-dimethylacetamide (DMAc 99.5% HPLC grade, Alfa Aesar) with 0.5% wt/vol lithium chloride (LiCl ACS 99%, Alfa Aesar) and left to dissolve for 24 h. Then, 100 μl of sample solution was injected into a SECcurity²-GPC system (PSS) equipped with a set of PSS GRAM columns (pre-column $10\text{ }\mu\text{m} \times 8 \times 50\text{ mm}$, 1 column $10\text{ }\mu\text{m} \times 30\text{ }\mu\text{m} \times 8 \times 300\text{ mm}$ and 2 columns $10\text{ }\mu\text{m} \times 1000\text{ }\mu\text{m} \times 8 \times 300\text{ mm}$) all maintained at 60°C . The eluent DMAc/LiCl was maintained at a flow rate of $1\text{ ml}/\text{min}$ with an isocratic pump. A RID detector was set at 35°C . The calibration with PSS ReadyCal-kit Poly(methyl methacrylate) and WinGPC UniChrom Software were used for the M_w estimation.

For (2) 3 mg of sample was dissolved in 1 ml of tetrahydrofuran (THF, for HPLC $\geq 99.9\%$, Sigma Aldrich) and left to dissolve for 24 h. Although THF cannot dissolve aged CN, it can readily dissolve camphor, which is the focus of this analysis. A volume of 50 μl sample solution was injected into a SECcurity²-GPC system (PSS) system with THF eluent flow at 1 ml/min. A set of PSS SDV columns (a pre-column 3 μm 8 \times 50 mm and 3 columns 3 μm 1000 \AA 8 \times 300 mm) were used and maintained at 25°C. The PSS ReadyCal-kit Poly(styrene) was used for the standard/internal calibration. For camphor quantification, an external calibration curve was obtained from five concentrations of pure camphor (Sigma-Aldrich) ranging from 1 to 2.5 g/L in THF, and analyzed with RID and UV detectors.

4 | AIM 1: EVALUATION OF ANALYTICAL TECHNIQUES

4.1 | Results and discussion

4.1.1 | Thermogravimetric analysis coupled with infrared spectroscopy

Characterizing decay products

The TGA-curves of the reference materials are shown in Figure 4. The samples R-g and R-m show a single-step decomposition (3) at 191 and 194°C, respectively (Table 1). R-s shows two steps of mass loss: in the first step the sample lost $4.3\% \pm 0.1\%$ of its weight up to 88°C and in the second, it lost another $9.5\% \pm 1.9\%$ of its weight up to 147°C, before its organic decomposition at

185°C. For R-s, when compared to R-g and R-m, the release of gases at lower temperatures, appeared to be connected to its severe condition.

The museum samples M-1-3 show one or two mass loss steps before decomposition (Figure 5). Their values show a similar trend to the R-s values. It is reasonable to assume that degradation processes, such as hydrolysis of the nitro groups and chain scission, lead to an earlier emission of thermal decay products on R-s and M-1-3. These samples denote a decrease in mass loss at decomposition temperature and an increase of residue at the end of analysis when compared with the less aged samples (R-g and R-m). Such an increase of residues is attributed to a higher percentage of nonvolatile carbonaceous material remaining in the crucible after pyrolysis, which has also been previously documented for pure CN without any additives.²⁵

The evolved gases resulting from all samples during the steps (1), (2) and (3) were analyzed by means of FTIR. In Table 2 the detected components are listed. Assignments of the IR bands to vibrational modes of atomic groups are shown in Table 3. As pointed out from the thermal analysis, the samples R-g and R-m did not emit any gases before their decomposition. For samples R-s, M-1, M-2, and M-3, instead, an early release of gases composed of camphor, H₂O and CO₂, was detected during their first mass loss step. These were followed by N₂O in the second mass loss step for M-1 and M-2, whereas R-s showed nearly the same gases in both the second and third steps. In step 3 the signal of N₂O for R-s is either missing, possibly due to the loss of N-O bonds during aging (see sec. Characterizing the hydrolysis of nitro groups), or is below the instrument's detection limit.

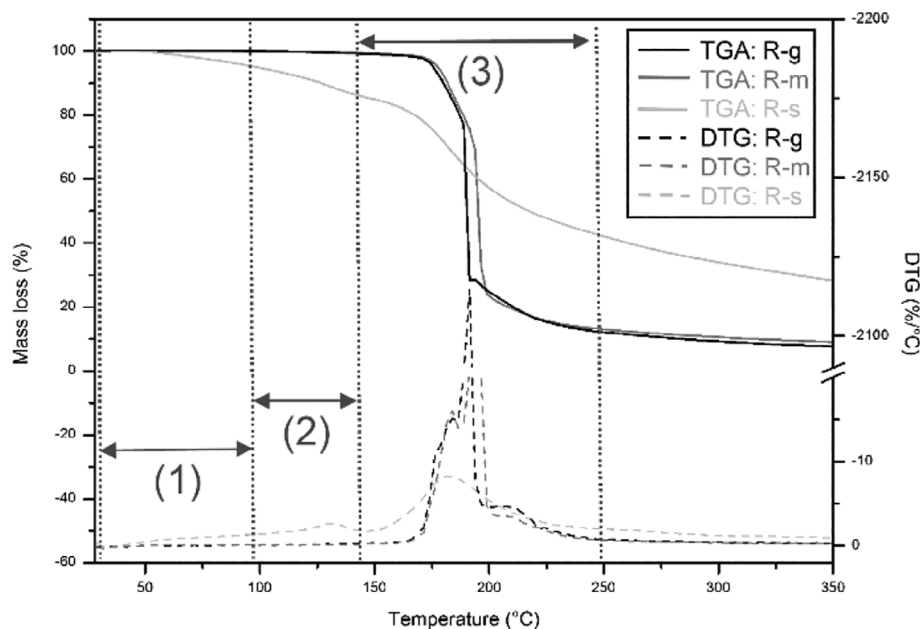


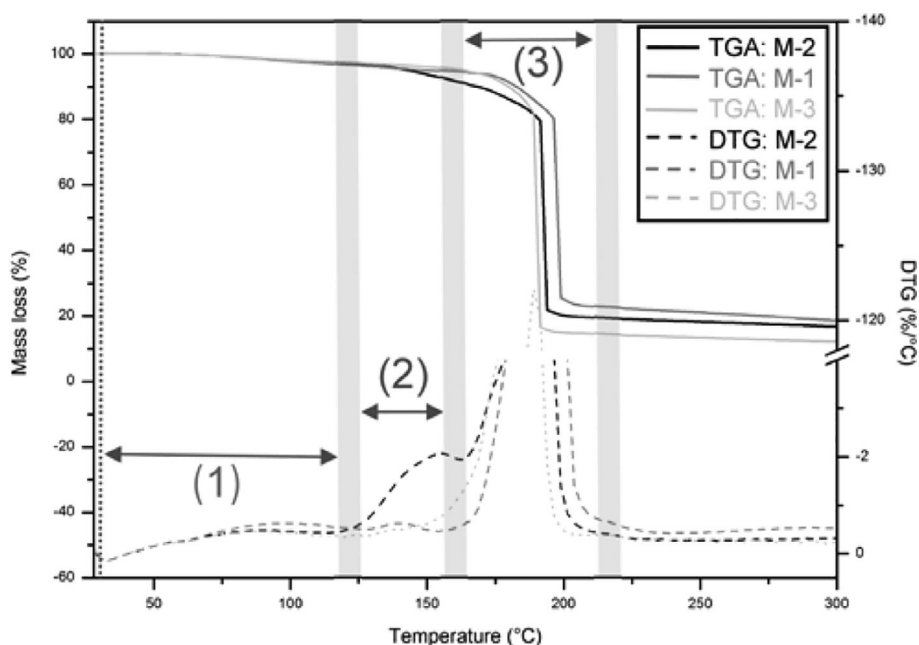
FIGURE 4 Thermogravimetric analysis (TGA)-DTG curves of the reference material divided in three steps: (1) First mass loss step; (2) second mass loss step; (3) organic decomposition. The samples R-g and R-m show a single-step (3), whereas R-s also shows steps (1) and (2) (with $4.3\% \pm 0.1\%$ and $9.5\% \pm 1.9\%$ mass loss respectively) before step (3)

TABLE 1 Results of the TGA-FTIR analysis

Sample	Mass loss step (1)		Mass loss step (2)		Organic decomposition (3)		Residue at 550°C mass (%)
	T _{max peak} (°C)	Mass loss (%)	T _{max peak} (°C)	Mass loss (%)	T _{max peak} (°C)	Mass loss (%)	
R-g	/	/	/	/	191 ± 1.0	84.7 ± 2.3	6.5 ± 1.8
R-m	/	/	/	/	194 ± 1.2	85.0 ± 3.5	7.5 ± 2.7
R-s	65 ± 3.1	4.3 ± 0.1	130 ± 3.1	9.5 ± 1.9	185 ± 1.2	64.3 ± 1.4	19.5 ± 0.6
M-1	98 ± 5.7	3.8 ± 0.2	131 ± 2.6	1.6 ± 0.2	197 ± 5.5	70.1 ± 1.8	13.2 ± 1.5
M-2	89 ± 1.0	2.6 ± 0.2	147 ± 9.8	6.0 ± 2.3	191 ± 6.2	68.9 ± 5.3	12.5 ± 2.2
M-3	87 ± 0.6	2.6 ± 0.1	/	/	188 ± 1.7	81.1 ± 0.7	8.3 ± 0.3

Abbreviation: TGA-FTIR, thermogravimetric analysis coupled with Fourier transform infrared spectroscopy.

FIGURE 5 Thermogravimetric analysis (TGA)-DTG curves of the naturally aged museum celluloid samples. At the first mass loss step (1) samples M-1, M-2 and M-3 lost 3.8%, 2.6% and 2.6% of their weight, respectively. At the second mass loss step (2), M-1 lost 1.6% and M-2 6.0%, while M-3 showed no additional loss step. The museum samples lost between 69–81% mass during their organic decomposition (3)

**TABLE 2** Evolved gases during TGA-FTIR analysis

Sample	Mass loss step (1)	Mass loss step (2)	Organic decomposition (3)
R-g	/	/	a, b, c, d, e, f, g
R-m	/	/	a, b, c, d, e, f, g
R-s	a, b, c	a, b, c, d, e, f, g	a, b, c, e, f, g
M-1	a, b, c	a, b, c, d	a, b, c, d, e, f, g
M-2	a, b, c	a, b, c, d	a, b, c, d, e, f, g
M-3	a, b, c	/	a, b, c, d, e, f, g

Note: a, camphor (C₁₀H₁₆O); b, water (H₂O); c, carbon dioxide (CO₂); d, nitrous oxide (N₂O); e, carbon monoxide (CO); f, nitric oxide (NO); g, formic acid (HCOOH).

Abbreviation: TGA-FTIR, thermogravimetric analysis coupled with Fourier transform infrared spectroscopy.

It has been documented in the literature that the organic decomposition of pure CN results in the evolution of H₂O, CO₂, CO, HCOOH, N₂O, NO, NO₂ and HCHO.^{28–30} This study confirms such results with the addition of camphor and the exception of NO₂ and

HCHO. Camphor is present due to the fact that the samples are made of celluloid. The reason why NO₂ and HCHO could not be detected may be attributed to their respective bands at 1630–1598 and 1771–1720 cm⁻¹ overlapping the frequencies of H₂O and HCOOH. Another

TABLE 3 Assignments of the IR bands to molecular functional groups used for TGA-FTIR analysis

Component	Frequency range (cm ⁻¹)	Functional group	Reference
Water, H ₂ O	3980–3480	O–H	28,49,50,51,52
	1980–1321	O–H	
Camphor, C ₁₀ H ₁₆ O	2966	C–H	52
	2891	C–H	
	1760	C=O	
Carbon dioxide, CO ₂	2361	C=O	28,49,50,52,53
	2344	C=O	
	671	C=O	
Carbon monoxide, CO	2178	C≡O	30,49,50,51,52,53
	2113	C≡O	
Nitrous oxide, N ₂ O	2238	N–N	30,50,51,54
	2209	N–N	
Nitric oxide, NO	1907	N=O	28,30,50,51,54
	1875	N=O	
Formic acid, HCOOH	1792	C=O	28,30,49,51
	1758	C=O	
	1122	C–O	
	1088	CH	
Nitrogen dioxide, NO ₂	1630	NO ₂	28,53,50,54
	1598		
Formaldehyde, HCHO	2804	CH ₂	28,30,51
	1771	CO	
	1749	CO	
	1718	CO	
	1504	CH ₂	

Abbreviation: TGA-FTIR, thermogravimetric analysis coupled with Fourier transform infrared spectroscopy.

reason may be associated with the interaction between NO₂ and HCHO during the TGA-FTIR analysis, based on the following reaction^{28–29,55}:



Characterizing the hydrolysis of nitro groups

Given that one of the most significant processes in the degradation of CN is the hydrolytic splitting of –O–NO₂ bonds, which results in a decrease of nitrogen content, it is assumed that these bonds would be the first to be affected by the thermal aging. This process can be monitored considering the reference materials before (R-g) and after severe aging (R-s). In the 3D FTIR spectra (Figure 6) R-s showed a lower intensity of all emitted gases over a broader temperature range

compared to R-g. For a better understanding of the concentration of released nitro gases and monitoring their reduction, their integration was performed; the areas of bands N₂O at 2238 cm⁻¹ and NO at 1907 cm⁻¹ were integrated over the total temperature range (Figure 7).

The integration highlights similar trends for both samples, as evidenced by the previous TGA results. While the evolution of N₂O and NO from R-g is limited to a narrow temperature range around its thermal decomposition (160–247°C), the same signals originating from R-s are distributed over a broader temperature range (90–265°C) and are, in general, less intense. Two peaks in particular, at 135 and at 199°C, are observed for NO, corresponding to the second mass loss step and the thermal decomposition of R-s, respectively. Instead, the signal of N₂O, is only present during the second mass loss step, between 100 and 180°C.

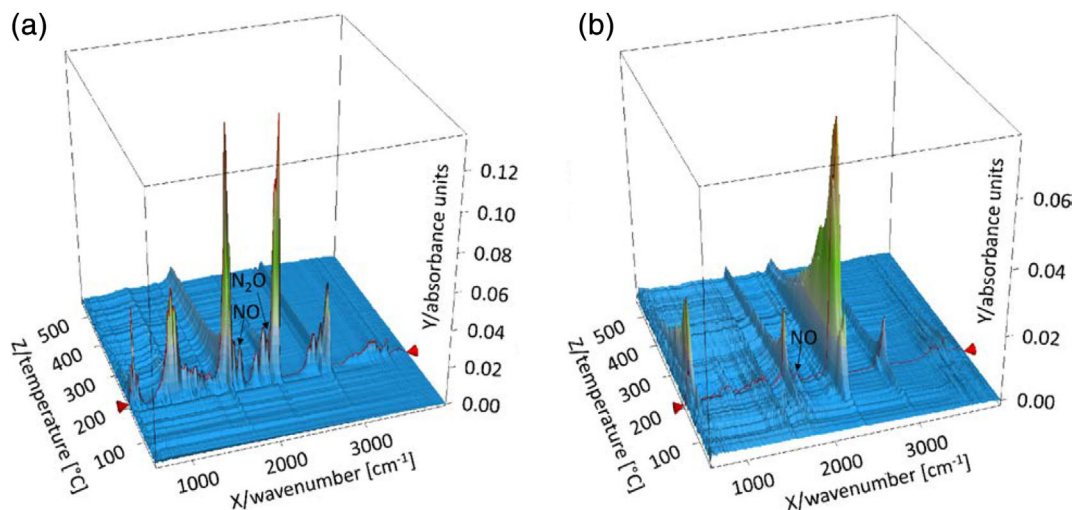


FIGURE 6 3D Fourier transform infrared (FTIR) spectra of evolved gases emitted by R-g (a) and R-s (b) during the thermogravimetric analysis (TGA) analysis. The organic decomposition is highlighted in red. The absorbing intensity of the characteristic bands of N_2O and NO showed a decrease in R-s, compared to R-g and in the organic decomposition N_2O could not be detected for R-s [Color figure can be viewed at wileyonlinelibrary.com]

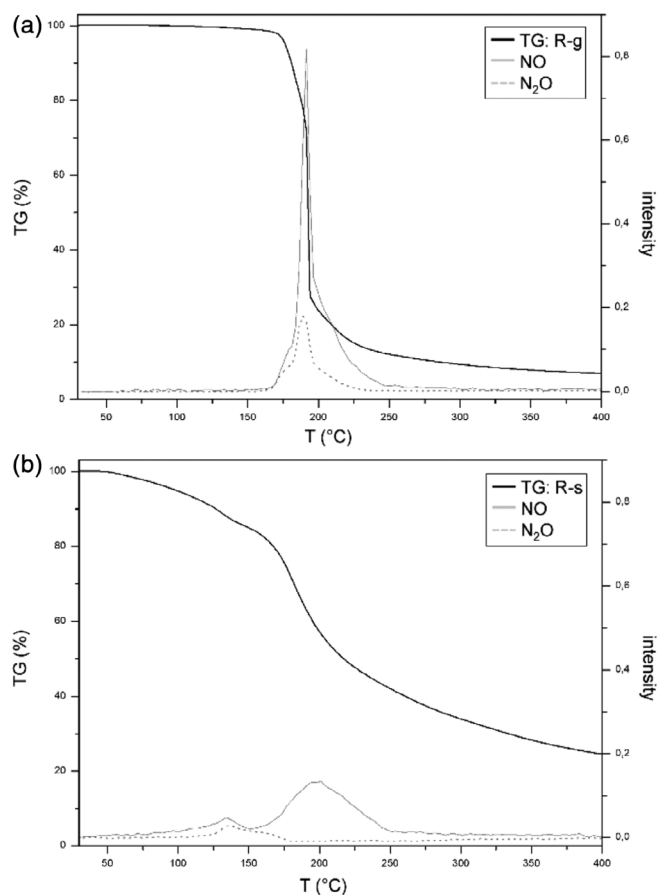


FIGURE 7 Intensity distribution of N_2O and NO for R-g (a) and R-s (b)

Table 4 reports the intensity of N_2O and NO calculated by integration of their respective absorption bands. The severely aged R-s showed less than half of the N_2O

signal of the unaged R-g, while the intensity of NO signal was decreased by more than one third from R-g to R-s. These results indicate a clear reduction of the nitro groups for R-s due to artificial aging.

A quantification of the nitrogen content with the applied method was not possible, because the signals of N_2O and NO in the respective region of 2209 and 1875 cm^{-1} overlap the absorption bands of CO and HCOOH. In forthcoming studies the authors will employ Ion chromatography to quantify the nitrogen content of natural and artificial aged celluloid.

4.1.2 | Evolved gas analysis–Mass spectrometry

Characterizing decay products

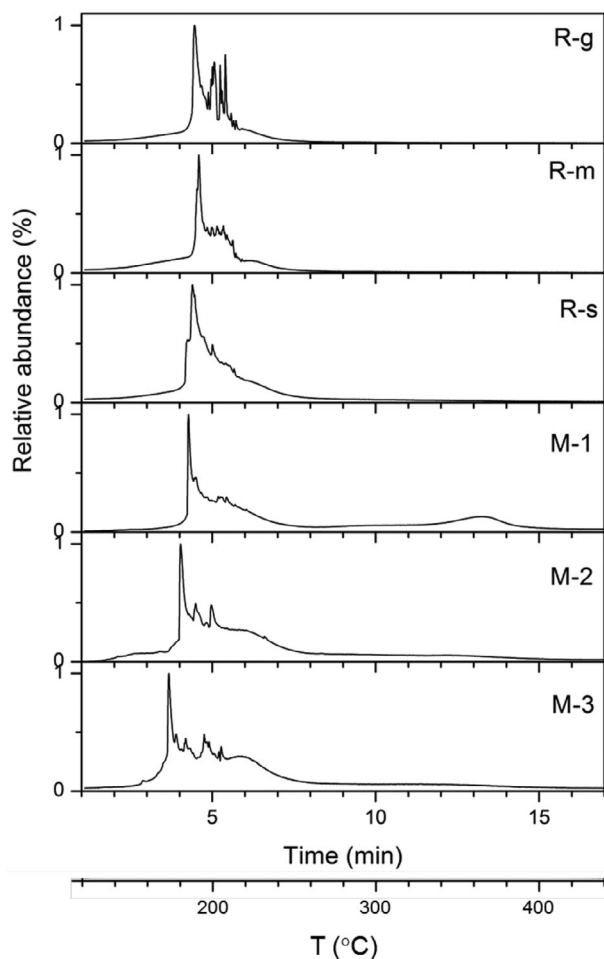
Figure 8 shows the thermograms of all reference and naturally aged samples. Unlike other esters of cellulose, EGA analysis of celluloid produces thermogram without clear thermal decomposition zones for cellulosic components.^{36,56} The gas emission of R-g and R-m is in the temperature range between 188 and 240°C. The EGA curve of R-s shows another trend, the evolved gas started to be released at a lower temperature, around 183°C, and lasted up to 260°C. This tendency was also observed in naturally aged samples; M-1, M-2 and M-3 emitted evolved gas between 185 and 500°C, 172–420°C and 160–500°C, respectively.

In order to understand this phenomenon, selected ion curves of the main volatiles, previously detected with TGA-IR analysis, were extracted (Figure 9). The first

TABLE 4 Calculated intensity of nitrous oxide and nitrogen dioxide

Sample	FTIR-intensity N ₂ O (a.u.)	FTIR-intensity NO (a.u.)
R-g	20.4 ± 0.2	68.56 ± 0.78
R-s	7.8 ± 0.4	42.1 ± 9.5

Abbreviation: FTIR, Fourier transform infrared spectroscopy.

**FIGURE 8** Normalized evolved gas analysis (EGA)-thermograms in total ion current for all celluloid reference and naturally aged samples

volatile released from celluloid samples was camphor (m/z 152), followed by NO (m/z 30), CO₂ (m/z 44), N₂O (m/z 44), NO₂ (m/z 46), and formic acid (m/z 46). As reported by Schilling et al.³⁶ the detection of nitro compounds (NO, N₂O and NO₂) after the emission of camphor (around 200–250°C) is indicative of celluloid pyrolysis degradation, excluding external contamination (e.g. air leakage). Compared to R-g, R-s is characterized by a broader range of temperature at which gases evolve, particularly camphor (m/z 152) starts earlier. This

compound together with CO₂/N₂O (m/z 44) show a prolonged emission. Moreover, the ratio between these two ions changed: in case that the ion m/z 152 is more abundant in R-g, then in R-s the ion m/z 44 becomes more dominant. This observation is also valid for the naturally aged samples M-2 and M-3 and it could be related to the loss of plasticizer due to aging. These two museum samples are characterized by an earlier release of evolved gases, mainly composed by CO₂ and camphor, and a dominant release of CO₂ after the evaporation of the plasticizer. The sample M-2 presents also a shorter temperature range of evolved gas emission in comparison with the other museum samples, possible due to presence of pigment(s) (not investigated)–in its formulation. Different behavior presents the sample M-1, after a similar release of both CO₂ and camphor at lower temperature (185°C) and the main evolution of camphor, the sample is then characterized by a long evolved gas release until 500°C of mainly CO₂ as well as a further camphor peak between 340 and 380°C. This could be related with the natural aging of the object, as for example, cross-linking between the chains, which would difficult the release of camphor from cross-linked polymer regions only at higher temperatures.

4.1.3 | Double shot – Gas chromatography/mass spectrometry

Characterizing decay products

The complete list of volatiles (Table S1) and pyrolytic products (Table S2) are reported in the Supporting Information. Figures 10 and 11 show the thermal desorption (TD-GC/MS) and flash pyrolysis (Py-GC/MS) of all samples. In the first step of the analysis (TD-GC/MS) several decay products from both the camphor and the cellulosic matrix were detected (Table 5). While no volatiles were detected for R-g, a few compounds, such as acetaldehyde and d-camphoric anhydride, were identified for R-m. R-s was characterized by an increase in formic acid and the appearance of furfural, 2(5H)-furanone, levoglucosanone and 1,4:3,6-dianhydro- α -d-glucopyranose. The naturally aged samples presented similar volatiles as R-s; furfural, levoglucosanone and 1,4:3,6-dianhydro- α -d-glucopyranose. Camphene was additionally identified for M-1. The detection and increase of furfural with aging suggests that this compound acts as a degradation marker for celluloid objects, in line with Curran et al.⁵⁷ Other volatiles, including acetaldehyde and formic acid, are typical degradation compounds of cellulose, especially at lower temperatures (100–200°C).⁵⁸

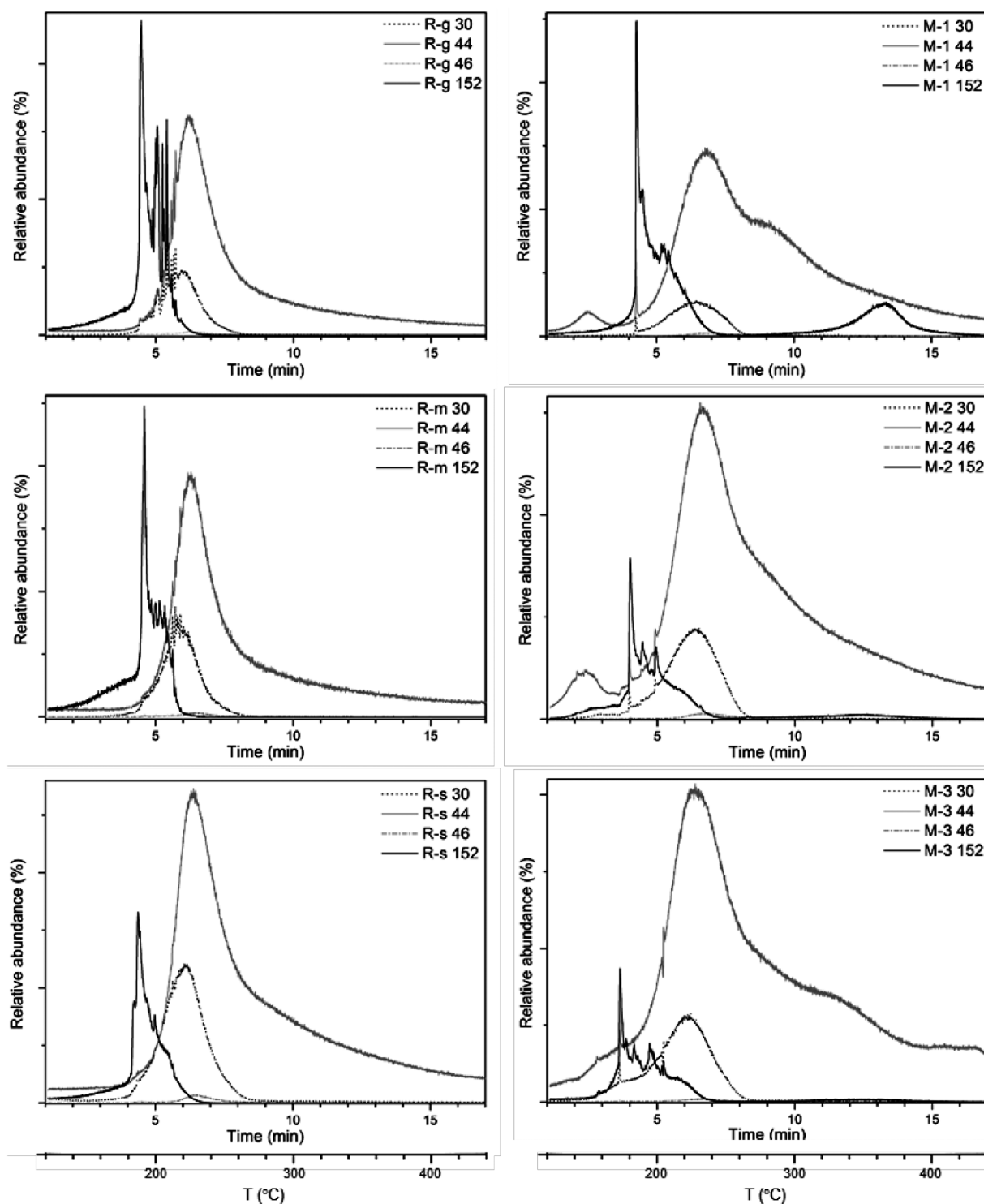


FIGURE 9 Extracted curves at m/z 30 (NO), m/z 44 ($\text{CO}_2/\text{N}_2\text{O}$), m/z 46 ($\text{NO}_2/\text{formic acid}$) and m/z 152 (camphor) for all reference and naturally aged samples. The curves are scaled to the largest peak in each plot

The decay products characterized in the second step of the analysis (Py-GC/MS) are reported in Table 6. Unaged R-g showed no decay products, whereas moderately aged R-m only emitted furan-2-propyl. Furan-2,5-dimethyl, 2-vinylfuran, furan-2-methyl, succinaldehyde, 5-(hydroxymethyl)-2-furfural, levoglucosan and 1,6-anhydro-

β -D-glucofuranose were detected in severely aged R-s. As previously observed in the first step of the analysis, naturally aged samples showed a similar degradation pattern to the artificially aged samples, with the additional detection of acetaldehyde, (3,3-dimethylcyclohexylidene) from camphor.

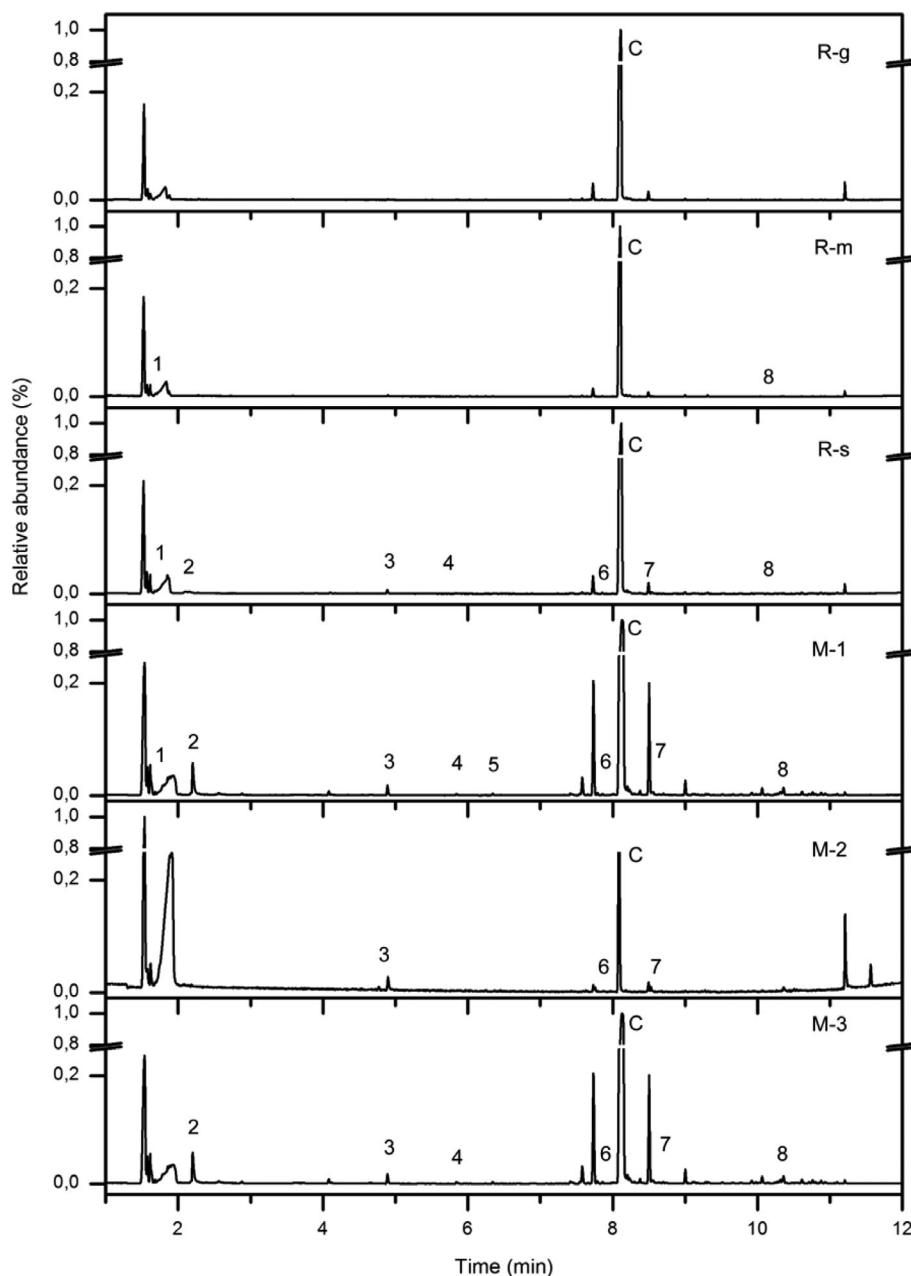


FIGURE 10 Normalized thermal desorption chromatograms (total ion chromatograms) of celluloid reference and naturally aged samples. For peak identification see Table 4 (C refers to camphor)

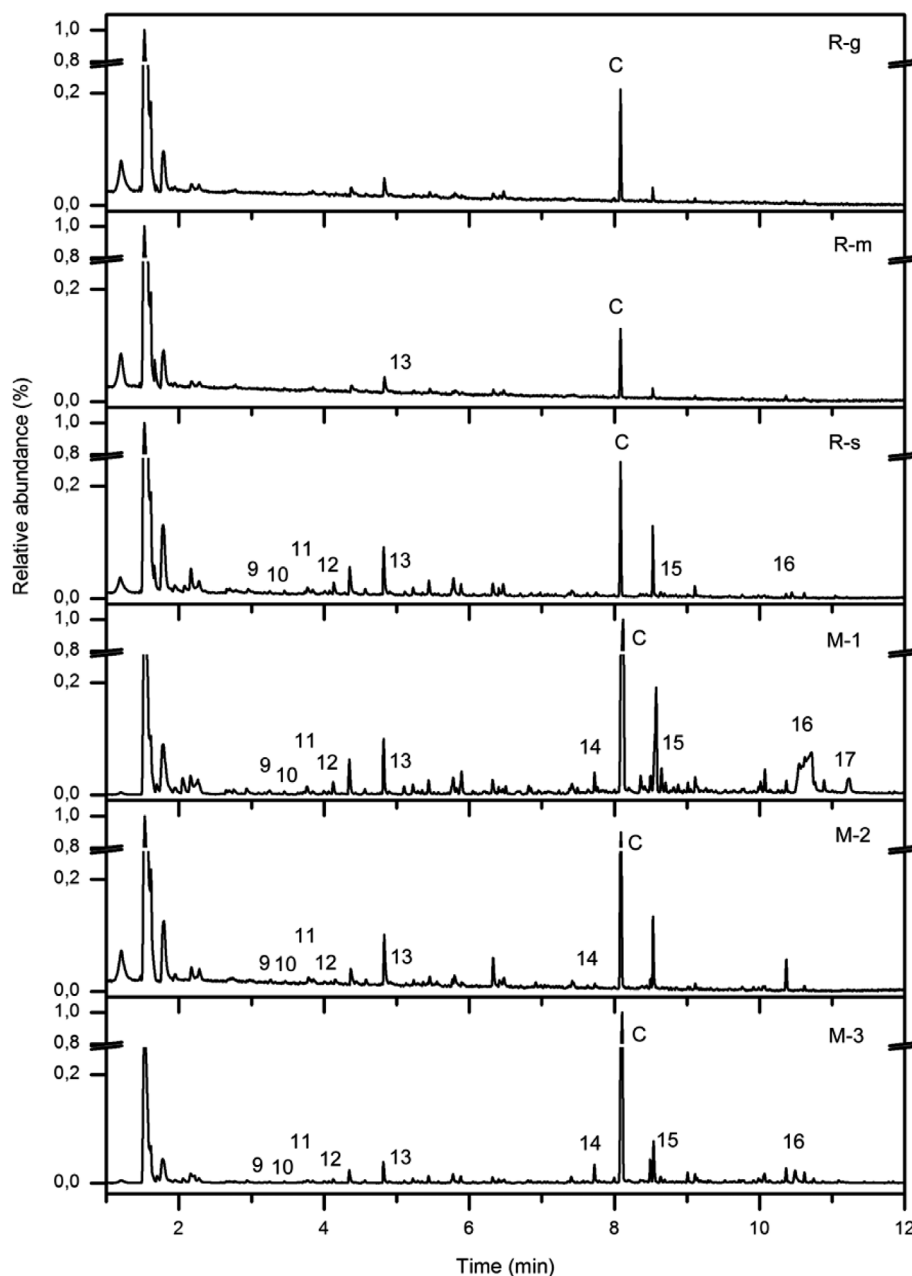
These results confirm that the unaged R-g and the moderately aged R-m still have their original, or almost intact, nitrogen content from production (estimated to be around 7–11%)⁵⁹ and produced none or a few decay products typical of pyrolysis of nitrocellulose.⁶⁰ While the aged samples (R-s, M-1-3) probably lost nitro groups during (artificial or natural) aging and behaved similarly to cellulose.^{10,58,61}

Estimating camphor content

The peak of camphor was detected in both TD and Py chromatograms of all samples (Figures 10 and 11). As previously highlighted by EGA-MS analysis, R-s emitted a broader range of evolved gases than R-g, including

camphor (m/z 152). Even if its presence was not quantified, it was detected in significant amounts, also in the degraded museum samples, as observed by Mazurek et al.¹² A semi-quantitative ratio was calculated for each sample, dividing the peak area of camphor detected during the first step (TD-GC/MS) with that obtained during the second step (Py-GC/MS). As reported in Table 7, R-g and R-m show a high camphor ratio (125) because the amount of camphor detected in the first step (until 220°C) is much higher than that left in the CN matrix and detected in the second step (at 600°C). For aged samples (artificially/naturally), the camphor ratio decreases (34 or ca. 2) because aged samples, which tend to start emitting volatiles at lower temperatures, also keep

FIGURE 11 Normalized pyrograms (total ion chromatograms) of celluloid reference and naturally aged samples. For peak identification, see Table 5 (C refers to camphor)



emitting them at higher ones when compared with fresh samples (as mentioned in the sec. 4.1.2). The camphor ratio shows a trend that can be useful to relatively compare the degradation level of artificially aged samples.

4.1.4 | Gel permeation chromatography

Characterizing chain scission

The M_w tended to decline for aged samples indicating their decomposition. As reported in Table 8, the M_w value of the reference sample heavily decreased from 222,000 (R-g) to 24,900 Da (R-s; ca. 11% of the original value) after artificial aging. The values of R-s fit well with those of M-1-3 (M_w range 17,000–24,100 Da) and those

reported in the literature for naturally aged celluloid in museum collections (M_w range 14,175–80,370 Da).^{8,12} As a result of chain scissions such materials have weakened and become progressively embrittled.

Estimating camphor content

The expected camphor concentration of new celluloid products ranges between 20–33% w/w, which was in accordance with the value of R-g (27%).^{5,7,15,18} After artificial aging, the camphor content was reduced by ca. 50% (see R-s - Table 8), reaching a value closer to that of the museum samples in the range of 13.5–17.7%.

The loss of plasticizer causes great changes in the physical properties of the polymer, resulting in embrittlement, which is, in turn, associated with the formation of

TABLE 5 Identification of volatile decay products obtained during the thermal desorption analysis of celluloid reference and naturally aged samples (characteristic ions in mass spectra: M_w in bold and base peak underlined)

Label	RT	Assignment of main peaks	m/z	R-g	R-m	R-s	M-1	M-2	M-3
1	1.67	Acetaldehyde (90% in F-Search, 77.4% in NIST)	<u>29</u> , 42, 43, 44	—	x	x	x	—	—
2	2.20	Formic acid (83.8% in NIST)	18, 28, 29, 44, 45, 46	—	—	x	x	—	x
3	4.89	Furfural (99% in F-search, 76.2% in NIST)	29, 39, 67, 95, 96	—	—	x	x	x	x
4	5.83	2(5H)-Furanone (83.7% in NIST)	27, 39, <u>55</u> , 84	—	—	x	x	—	x
5	6.24	Camphene (27.7% in NIST)	27, 39, 53, 67, 79, <u>93</u> , 107, 121, 136	—	—	—	x	—	—
6	7.75	Levoglucosanone (87% in NIST)	29, 39, 53, <u>68</u> , 81, 98, 126	—	—	x	x	x	x
7	8.53	1,4:3,6-dianhydro- α -D-glucopyranose (95.1% in NIST)	29, 41, 57, <u>69</u> , 86, 98, 114, 127, 144	—	—	x	x	x	x
8	10.38	d-Camphoric anhydride (34.4% in NIST)	27, 41, 55, 69, 83, <u>95</u> , 110, 123, 138, 182	—	x	x	x	—	x

TABLE 6 Identification of decay products by flash pyrolysis of celluloid reference and naturally aged samples (characteristic ions in mass spectra: M_w in bold and base peak underlined)

Label	RT	Assignment of main peaks	m/z	R-g	R-m	R-s	M-1	M-2	M-3
9	3.25	Furan-2,5-dimethyl (74.5% in NIST)	27, 43, 53, 67, 81, 96	—	—	x	x	x	x
10	3.46	2-Vinylfuran (45.7% in NIST)	27, 39, 65, 94	—	—	x	x	x	x
11	3.77	Furan-2-methyl (84% in F-Search, 68.8% in NIST)	27, 39, 53, 82	—	—	x	x	x	x
12	4.13	Succindialdehyde (68.7% in NIST)	29, 43, <u>58</u> , 86	—	—	x	x	x	x
13	5.22	Furan-2-propyl (84.2% in NIST)	27, 53, <u>81</u> , 110	—	x	x	x	x	x
14	7.72	Acetaldehyde, (3,3-dimethylcyclohexylidene)-, E- (28.5% in NIST)	41, 55, 69, 81, 95, <u>108</u> , 137, 152	—	—	—	x	x	x
15	8.64	5-(Hydroxymethyl)-2-furfural (92% in F-search, 86.6% in NIST)	29, 41, 53, 69, 81, <u>97</u> , 109, 126	—	—	x	x	—	x
16	10.49	Levoglucosan (99% in F-search, 48.2% in NIST)	43, 57, <u>60</u> , 73, 98, 162	—	—	x	x	—	x
17	11.23	1,6-anhydro- β -D-glucofuranose (67.2% in NIST)	29, 44, 57, 69, <u>73</u> , 85, 98, 115, 162	—	—	x	x	—	—

TABLE 7 Camphor ratio calculated between the peaks areas of camphor obtained from the first (TD-GC/MS) and second (Py-GC/MS) steps of the analysis of reference and naturally aged samples ($n = 2$)

	R-g	R-m	R-s	M-1	M-2	M-3
Camphor ratio	125.6 \pm 4.5	124.9 \pm 12.7	34.0 \pm 27.8	1.9 \pm 0.4	1.7 \pm 0.5	2.6 \pm 0.3

Note: The peaks considered for the area calculation were not normalized.

Abbreviations: Py-GC/MS, flash pyrolysis gas chromatography/mass spectrometry; TD-GC/MS, thermal desorption gas chromatography/mass spectrometry.

cracks and crazing. The decrease of the camphor content due to sublimation is a well-known degradation process for celluloid objects.^{7,8} This is possible because the camphor molecules are not chemically bound to each other and they can sublime and migrate out of and through CN.⁶² Starting with around 30% wt/wt camphor at production, this concentration has been documented to decrease after 30–40 years of natural aging until it reaches a constant level of 15%.^{7,15} Our results also show a camphor content of around 15% for naturally aged samples, which could indicate that besides sublimation, camphor molecules may be retained in the CN matrix during aging, perhaps due to degradative radical reactions. Even

though no literature was found to corroborate this hypothesis, further studies on this topic should be made.

4.1.5 | Comparison of analytical techniques for studying celluloid

Regarding the selection of thermal, spectroscopic, spectrometric and chromatographic methods for being the most suitable in characterizing celluloid decay products and assessing material changes due to degradation, the following conclusions were drawn and are summarized in Table 9:

TGA-FTIR: This technique is suitable for quantifying the temperature-dependent mass loss of celluloid samples and simultaneously identifying the evolved gases. The thermal analysis and FTIR detector allowed to differentiate the samples, especially the unaged reference material from the severely artificially aged and from the naturally aged museum celluloid. Although TGA-FTIR analysis was not as sensitive in detecting decay products as TD/Py-GC/MS, it was the only method with which the hydrolysis of nitro groups could be monitored. However, a limitation of this method was that quantification of a single component (e.g. camphor, nitro groups) was not possible due to an overlapping with other evolved gases. Therefore, further studies are needed to achieve quantification of the plasticizer (i.e. testing the application of an isotherm).

EGA-MS: This method is very useful as a starting point for understanding the composition of samples and highlighting differences in their condition when comparing samples with increasing aging. The EGA-MS results confirmed TGA-FTIR analysis, especially concerning the release of volatiles at lower temperatures from the more

degraded samples. The MS detector allowed the analysis to follow the evolution of specific celluloid markers, such as NO₂ and N₂O, or camphor, but not to quantify them.

TD/Py-GC/MS: this is a powerful technique for sample characterization, in which two analyses, thermal desorption and pyrolysis, are applied consecutively. TD/Py-GC/MS detected 13 different decay products from camphor and cellulose, including acetaldehyde, d-camphoric anhydride, formic acid, furfural, 2(5H)-furanone, levoglucosanone and 1,4:3,6-dianhydro- α -d-glucopyranose, which the previous techniques did not manage to identify.

Although camphor quantification was not investigated, a ratio between its peaks obtained by both TD-GC/MS and Py-GC/MS analyses was calculated. This ratio can be ultimately used to relatively compare the degradation level of celluloids during artificially aging studies.

GPC: This is the most suitable method for studying even small material changes in celluloid samples within a time span, since it offers quantitative data that allow the comparison of M_w values before and after an event, in our case the artificial aging. Moreover, a different instrumental set-up than the one used for M_w measurements, allowed the quantification of camphor, revealing the versatility of this technique.

TABLE 8 Average molecular weight (M_w) of the reference and the naturally aged samples analyzed with DMAc + LiCl and their relative camphor amounts detected with THF

Samples	M _w	Camphor (%)
R-g	222,000 ± 1800 (n = 2)	26.9 ± 0.6 (n = 2)
R-m	189,000 ± 37,000 (n = 2)	17.2 ± 8.3 (n = 2)
R-s	24,900 ± 3000 (n = 2)	14.4 ± 5.7 (n = 2)
M-1	17,000 (n = 1)	17.7 ± 6.2 (n = 5)
M-2	24,100 (n = 1)	13.5 ± 5.9 (n = 2)
M-3	18,000 (n = 1)	16.4 ± 4.4 (n = 5)

Abbreviations: DMAc, N,N-dimethylacetamide; LiCl, lithium chloride; THF, tetrahydrofuran.

4.1.6 | Assessment of material changes and decay products in the samples

By comparing all the techniques studied here, it became evident that the unaged (R-g) and the moderately artificially aged reference (R-m) are chemically similar since they showed similar TGA-FTIR-curves, IR spectra at the decomposition point, average M_w values, and very few decay products as established through TD/Py-GC/MS analysis. This suggests that the moderate artificial aging

TABLE 9 Specifications of the analytical techniques implemented in this study for characterizing the decay products and assessing the material changes of celluloid

Analytical technique	Characterize decay products	Assess material changes associated with			Sample size	Pretreatment/preparation of the sample
		Hydrolysis of nitro groups	Loss of camphor	Chain scission		
TGA-FTIR	TGA Δ FTIR \circ	\oplus			10 mg	No
EGA-MS	\circ				~200 μ g	No
TD/Py-GC/MS	TD-GC/MS \circ Py-GC/MS \circ		\oplus		~100 μ g	No
GPC			Δ	Δ	3 mg	Yes

Note: Δ Quantitative; \circ Qualitative; \oplus Semi-quantitative approach (tendency).

Abbreviations: EGA-MS, evolved gas analysis–mass spectrometry; GPC, gel permeation chromatography; Py-GC/MS, flash pyrolysis gas chromatography/mass spectrometry; TD-GC/MS, thermal desorption gas chromatography/mass spectrometry; TGA-FTIR, thermogravimetric analysis coupled with fourier-transform infrared spectroscopy.

applied did not induce much chemical degradation to the reference material. On the contrary, after the severe artificial aging the reference sample was degraded by all three main degradation processes; hydrolysis, chain scission and loss of plasticizer. The sample R-s reached a condition comparable with the naturally aged museum samples (M-1-3) as confirmed by the decay products obtained from TD/Py-GC/MS analysis, as well as the M_w and camphor quantification by GPC. Among the museum objects, sample M-2 emitted few volatiles and decay products as observed during the TD/Py-GC/MS analysis. This could be attributed to the presence of pigments and/or fillers in its formulation that could have acted as stabilizers, slowing down the natural aging process.⁶³ However, a comparison between the naturally aged museum objects is not possible, due to their different periods of production, unknown original composition and degradation histories.

After artificial aging, the reference sample R-s decreased its M_w by ca. 90%, whereas the camphor content was reduced by ca. 50%. This observation could corroborate the hypothesis that the main degradation process was hydrolytic chain scission, resulting in loss of M_w , and that loss of camphor was less involved.^{8,62} Only a few studies have addressed the quantification of plasticizer, and mainly in other cellulose esters.^{12,64} The evolution of camphor and its content during the degradation of CN has not yet been studied in-depth. Further studies are necessary to better understand the chemistry between camphor and CN, particularly during aging.

5 | AIM 2: GPC ANALYSIS TO SHOWCASE THE HETEROGENEOUS NATURE OF DEGRADED CELLULOID

5.1 | Results and discussion

Within the first aim of this article, GPC was selected for its ability to quantitatively assess material changes in celluloid. These changes are associated with two main degradation processes: (i) the reduction of the chain lengths due to scission and (ii) the loss of plasticizer (camphor) due to sublimation. Since celluloid tends to degrade heterogeneously, in this second part of the article, GPC will be applied with two different set ups to investigate differences in the M_w and camphor content of degraded CN areas with distinct characteristics. An artificially and a naturally aged sample were studied for this purpose. Two sampling points were obtained from each sample: one area appeared macroscopically without physical

TABLE 10 Average molecular weights (M_w) and camphor content of the celluloid samples with different degradation areas analyzed with GPC ($n = 3$)

Samples	M_w	Camphor (%)
P-g	305,000 ± 31,000	35.5 ± 1.1
P-n	178,000 ± 17,500	30.9 ± 1.9
P-d	61,900 ± 5400	30.8 ± 1.0
M1-n	50,200 ± 3400	31.4 ± 2.2
M1-d	14,700 ± 750	17.7 ± 6.2

Note: d, physical damage; g: unaged in good condition; M1, transparent plate, naturally aged museum celluloid sample; n, no physical damage; P, plate.

Abbreviation: GPC, gel permeation chromatography.

damages, while the other was visibly damaged, cracked or crazed (Figure 3).

As reported in Table 10, the average M_w value of the unaged P-g is within the range of new commercial celluloid products.^{15,16} After artificial aging, the average M_w of the area without physical damage (P-n) decreases to ca. 58% of the unaged value, whereas the average M_w of the area with crazes and bubbles (P-d), decreases to ca. 20% of the unaged value. The artificially aged sample shows a range of M_w values between 178,000–61,900 Da, which prove the inconsistent development of chain scissions in the polymer, associated with the heterogeneous nature of celluloid.

The naturally aged sample M1, shows a range of M_w values between 50,200 and 14,700 Da, similar to the naturally aged museum objects (M_w range 14,000–81,000 Da).^{8,12} The intervals between the average M_w values of aged celluloid denote the sensitivity of GPC in characterizing its heterogeneous nature.

Regarding the camphor quantification, the average value of 35% documented for the unaged sample decreases after artificial aging to 31% for both undamaged and damaged areas. Even though the loss of plasticizer is known to cause shrinkage and brittleness, which lead to the cracking of celluloid, results in this study suggest that loss of M_w is the major factor contributing to visible damage.^{7,8,65} For similar aging conditions (70°C and 75% RH) Quye et al.⁶³ observed that humidity plays an important role in the chain scission processes of celluloid. Observations in this study confirm that the applied artificial aging conditions strongly induced chain scission processes.

The naturally aged museum sample M1 displayed another tendency. A major difference in the camphor content was measured in both areas: the camphor content reached 31% for M1-n (without visible damage) and 18% for M1-d (with cracks and crazes),

showing a decrease of more than two fifth between the two areas.

As presented in this study chain scission and migration of camphor are not uniform processes across the celluloid samples. The quantification of M_w and camphor content with GPC are useful tools to characterize this heterogeneous nature of degraded celluloid and assist in the understanding of the different levels of degradation and the effects of artificial aging. However, GPC results for aged celluloid are strongly dependent on where the sample is collected. Therefore, much care should be taken, to document the sampling areas and procedures properly when assessing the effects of aging or conservation treatments in the laboratory.

6 | CONCLUSION

This study has demonstrated strengths and weaknesses of the applied analytical techniques for characterizing celluloid decay products and assessing the material changes attributed to hydrolysis of nitro groups, loss of camphor and chain scission.

TGA-FTIR, EGA-MS, and TD/Py-GC/MS were applied to characterize decay products, with TD/Py-GC/MS being the most sensitive method for analyzing evolved gases; however, in our application without quantifying them. TGA-FTIR detected the total mass loss of all evolved gasses, without quantifying the mass loss attributed to each component due to their overlapping (at similar evolving temperatures).

Concerning the assessment of material changes associated with the hydrolysis of nitro groups, TGA-FTIR showed limitations due to the inability to separate the evolved gases of interest from the others.

Regarding the loss of plasticizer, and developed for first time in this study, TD/Py-GC/MS was implemented semi-quantitatively. GPC was also applied innovatively here for camphor quantification through the use of an external calibration.

In regard to material changes attributed to chain scission, GPC was the only tested method able to quantify molecular weight changes of cellulose nitrate.

The study has highlighted the benefit of GPC to assess material changes attributed to loss of camphor as well as chain scission, associated with two of the main important degradation processes of celluloid. This versatile method also proved to be very suitable for characterizing the heterogeneous nature of degraded celluloid on areas that macroscopically show different levels of degradation.

To understand the complex degradation of celluloid and support research projects aiming at prolonging its

lifetime by exploring effective and sustainable storage conditions, GPC is suggested for studying the camphor content and molecular weight distribution of celluloid. For determining the nitrogen content, the authors plan to employ ion chromatography in forthcoming studies. As the degradation of celluloid is nonuniform and specific to the sampling area of the analyzed material, the effectiveness of treatments will also be likely location-dependent. Therefore, it is recommended that in future research studies assessing the camphor content, molecular weight distribution and nitrogen content of cellulose nitrate/celluloid, the location of samples is clearly documented. Material changes along the profile depth of celluloid offer new insights on its heterogeneous nature and the way the three degradation processes influence each other.

ACKNOWLEDGMENTS

This work was financially supported by the German Federal Environmental Foundation (Deutsche Bundesstiftung Umwelt - DBU), through the Cultural Heritage Projection Programme (Förderbereich 13 - Bewahrung und Sicherung national wertvoller Kulturgüter vor schädlichen Umwelteinflüssen) under the project *Cold storage of museum objects made of cellulose nitrate – mechanical stress versus chemical degradation* (grant agreement no. 34790/01). The authors thank Christoph Heiner for supplying the reference celluloid materials. Dr Kavda would like to thank the Deutsches Museum for funding her through the Scholar-in-Residence Program.

ORCID

Christina Elsässer  <https://orcid.org/0000-0002-0766-4841>

Anna Micheluz  <https://orcid.org/0000-0003-1073-1723>

Marisa Pamplona  <https://orcid.org/0000-0002-0266-3549>

Stefani Kavda  <https://orcid.org/0000-0002-8596-2430>

Peter Montag  <https://orcid.org/0000-0003-1590-0901>

REFERENCES

- [1] K. Kohlhepp, *Kunststoffe* **2005**, *05*, 22.
- [2] J. Nils, in *Plastikwelten* (Ed: S. Weißler), Elefant Press, Berlin **1985**, p. 17.
- [3] Williams, S., *CCI Notes 15/3*, Canadian Conservation Institute, Ottawa **1994**.
- [4] K. Kessler, in *Kölner Beiträge zur Restaurierung und Konservierung von Kunst- und Kulturgut*, Vol. 13 (Ed: F. Köln), Siegl, München **2001**, p. 139.
- [5] F. Waentig, *Kunststoffe in der Kunst. Eine Studie unter konservatorischen Gesichtspunkten*, Michael Imhof Verlag, Petersberg **2004**.

- [6] M. Coughlin, A. M. Seeger, in *Plastics. Looking at the Future and Learning from the Past* (Eds: B. Keneghan, L. Egan), Archetype Publication, London **2008**, p. 119.
- [7] Y. Shashoua, *Conservation of plastics. Material science, degradation and preservation*, Butterworth-Heinemann, Oxford **2008**.
- [8] A. Quye, D. Littlejohn, R. A. Pethrick, R. A. Stewart, *Polym. Degrad. Stab.* **2011**, *98*, 1369.
- [9] M. Derrick, D. Stulik, E. Ordonez, in *Saving the twentieth century: The Conservation of modern materials* (Ed: D. W. Gratton), Canadian Conservation Institute, Ottawa **1993**, p. 169.
- [10] K. Sutherland, C. Schwarzinger, B. A. Price, *J. Anal. Appl. Pyrolysis* **2012**, *94*, 202.
- [11] J. Salvant, K. Sutherland, J. Barten, C. Stringari, F. Casadio, M. Walton, *e-PS* **2016**, *13*, 15.
- [12] J. Mazurek, A. Laganà, V. Dion, S. Etyemez, C. Carta, M. R. Schilling, *J. Cultural Heritage* **2019**, *35*, 263. <https://doi.org/10.1016/j.culher.2018.05.011>.
- [13] Williams, S., *CCI Notes 15/1*, Canadian Conservation Institute, Ottawa **1997**.
- [14] M. Schilling, M. Bouchard, H. Khanjian, T. Learner, A. Phenix, R. Rivenc, *Acc. Chem. Res.* **2010**, *43*, 888.
- [15] C. Selwitz, *Cellulose Nitrate in Conservation*, Getty Conservation Institute, USA **1988**.
- [16] G. Wypych, *Handbook of Polymers*, ChemTec Publishing, Toronto **2012**, p. 58. <https://doi.org/10.1016/B978-1-895198-47-8.50002-3>.
- [17] G. Bonwitt, *Das Celluloid und seine Ersatzstoffe*, Dt. Verl.-Ges, Berlin **1933**.
- [18] V. E. Yarsley, W. Flavell, P. S. Adamson, N. G. Perkins, *Cellulosic Plastics. Cellulose Acetate, Cellulose Ethers, Regenerated Cellulose, Cellulose Nitrate*, Iliffe Books LTD, London **1964**.
- [19] L. Meier, in *Taschenbuch der Kunststoff-Additive*, Vol. 3 (Eds: R. Gaechter, H. Mueller), Carl Hanser Verlag, Munich **1990**, p. 341.
- [20] D. Braun, *Kleine Geschichte der Kunststoffe*, Vol. 2, Carl Hanser Verlag, Munich **2017**.
- [21] UCL IRIS, Research Activities. <https://iris.ucl.ac.uk/iris/browse/researchActivity/20282> (accessed December 23, 2020).
- [22] The Getty Conservation Institute, Projects: (accessed Dec. 23, 2020). https://www.getty.edu/conservation/our_projects/science/plastics/cellulose.html.
- [23] Deutsches Museum, Research (accessed Dec. 23, 2020). <https://www.deutsches-museum.de/en/research/forschungsbereiche/sammlungen/restaurierungsforsch/cold-storage-of-museum-objects/>
- [24] NEMOSINE Project. <https://nemosineproject.eu/> (accessed Dec. 23, 2020).
- [25] J. Rychlý, A. Lattuati-Derieux, L. Matisová-Rychlá, K. Csomorová, I. Janigoá, B. Lavédrine, *J. Therm. Anal. Calorim.* **2011**, *107*, 1267. <https://doi.org/10.1007/s10973-011-1746-8>.
- [26] E. Richardson, M. T. Giachet, M. Schilling, T. Learner, *Polym. Degrad. Stab.* **2014**, *107*, 231. <https://doi.org/10.1016/j.polymdegradstab.2013.12.001>.
- [27] A. McQueen, K. Mullen, H. Heckman, V. I. Kepley, M. K. Mahanthappa, *Investigation of Cellulose Nitrate Motion Picture Film and Associated Fire Risk*, University of Wisconsin, Madison, White Paper **2015**.
- [28] N. Zhao, J. Li, H. Gong, T. An, F. Zhao, A. Yang, R. Hu, H. J. Ma, *Anal. Appl. Pyrolysis* **2016**, *120*, 165. <https://doi.org/10.1016/j.jaap.2016.05.002>.
- [29] A. Benhammada, D. Trache, *Appl. Spectrosc. Rev.* **2019**, *55*, 1. <https://doi.org/10.1080/05704928.2019.1679825>.
- [30] Y. Guo, N. Zhao, T. Zhang, H. Gong, H. Ma, T. An, F. Zhao, R. Hu, *RSC Adv.* **2019**, *9*, 3927. <https://doi.org/10.1039/c8ra09632e>.
- [31] J. La Nasa, G. Biale, B. Ferriani, M. P. Colombini, F. Modugno, *J. Anal. Appl. Pyrolysis* **2018**, *134*, 562. <https://doi.org/10.1016/j.jaap.2018.08.004>.
- [32] A. Lattuati-Derieux, S. Thao-Heu, B. Lavédrine, *J. Chromatogr. A* **2011**, *1218*, 4498. <https://doi.org/10.1016/j.chroma.2011.05.013>.
- [33] I. Degano, F. Modugno, I. Bonaduce, E. Ribechini, M. P. Colombini, *Angew. Chem., Int. Ed.* **2018**, *25*, 7313. <https://doi.org/10.1002/anie.201713404>.
- [34] J. La Nasa, G. Biale, F. Sabatini, I. Degano, M. P. Colombini, F. Modugno, *Herit Sci* **2019**, *7*, 8. <https://doi.org/10.1186/s40494-019-0251-4>.
- [35] J. La Nasa, G. Biale, B. Ferriani, R. Trevisan, M. P. Colombini, F. Modugno, *Molecules* **2020**, *25*, 1705. <https://doi.org/10.3390/molecules25071705>.
- [36] Schilling, M. R., Learner T. J. S. In *Cultural Heritage/Cultural Identity: The Role of Conservation*, Proceedings of the 16th ICOM Committee for Conservation Triennial Meeting, Lisbon, Portugal, Sep. 19–23, 2011; ICOCC: Lisbon; **2011**.
- [37] The POPART Project, Preservation of plastic artefacts in museum collections. <http://popart-highlights.mnhn.fr/introduction/the-popart-project/index.html> (accessed Dec. 27, 2020).
- [38] H. D. Burgess, *Stud Conserv* **1982**, *27*, 85. <https://doi.org/10.1179/sic.1982.27.Supplement-1.85>.
- [39] P. Engel, L. Hein, C. Spiess Antje, *Biotechnol. Biofuels* **2012**, *5*, 77. <https://doi.org/10.1186/1754-6834-5-77>.
- [40] C. L. McCormick, P. A. Callais, B. H. Hutchinson, *Macromolecules* **1985**, *18*, 2394. <https://doi.org/10.1021/ma00154a010>.
- [41] M. Strlič, J. Kolar, *J. Biochem. Biophys. Methods* **2003**, *56*, 265.
- [42] G. Strobini, D. Ciechańska, D. Wawro, S. Boryniec, H. Struszczyk, S. Sobczak, *Fibres Text. East. Eur.* **2003**, *11*, 62.
- [43] S. N. Patkar, P. D. Panzade, *Anal. Methods* **2016**, *8*, 3210. <https://doi.org/10.1039/C5AY03012A>.
- [44] H. Zhang, Y. Zhang, H. Shao, X. Hu, *J. Appl. Polym. Sci.* **2004**, *94*, 598. <https://doi.org/10.1002/app.20732>.
- [45] L. Segal, *J. Polym. Sci., Polym. Chem.* **1968**, *21*, 267. <https://doi.org/10.1002/polc.5070210124>.
- [46] C. Holt, W. Mackie, D. B. Sellen, *Polymer* **1978**, *19*, 1421. [https://doi.org/10.1016/0032-3861\(78\)90094-0](https://doi.org/10.1016/0032-3861(78)90094-0).
- [47] E. J. Siochi, T. C. Ward, *J. Macromol. Sci., Part C* **1989**, *29*, 561.
- [48] M. Á. Fernández de la Ossa, M. López-López, M. Torre, C. García-Ruiz, *Trends Analyt Chem.* **2011**, *30*, 1740. <https://doi.org/10.1016/j.trac.2011.06.014>.
- [49] T. Xu, X. Huang, *Fuel* **2010**, *89*(9), 2185. <https://doi.org/10.1016/j.fuel.2010.01.012>.
- [50] M. Jin, N. Luo, G. Li, Y. Luo, *J. Therm. Anal. Calorim.* **2015**, *121*, 901. <https://doi.org/10.1007/s10973-015-4574-4>.
- [51] R. Wei, S. Huang, Z. Wang, C. Wang, T. Zhou, J. He, R. Yuen, J. Wang, *J. Therm. Anal. Calorim.* **2018**, *134*, 953. <https://doi.org/10.1007/s10973-018-7521-3>.

- [52] X. Xu, R. Pan, P. Li, R. Chen, *Appl. Biochem. Biotechnol.* **2020**, *191*, 1605. <https://doi.org/10.1007/s12010-020-03300-2>.
- [53] Y. Wu, Z. Yi, Y. Luo, Z. Ge, F. Du, S. Chen, J. Sun, *J. Therm. Anal. Calorim.* **2017**, *129*, 1555. <https://doi.org/10.1007/s10973-017-6387-0>.
- [54] F. Cataldo, O. Ursini, C. Cherubini, S. Rocchi, *Polym. Degrad. Stab.* **2012**, *97*, 1090. <https://doi.org/10.1016/j.polymdegradstab.2012.04.009>.
- [55] W. Wei, B. Cui, X. Jiang, *J. Therm. Anal. Calorim.* **2010**, *102*, 863. <https://doi.org/10.1007/s10973-010-0695-y>.
- [56] S. Tsuge, H. Ohtani, C. Watanabe, *Pyrolysis-GC/MS data book of Synthetic polymers. Programs, thermograms and MS of polymers*, Elsevier, Oxford **2011**.
- [57] K. Curran, M. Underhill, J. Grau-Bové, T. Fearn, L. T. Gibson, M. Strlič, *Angew. Chem., Int. Ed* **2018**, *57*, 7336.
- [58] A. M. Emsley, G. C. Stevens, *Cellulose* **1994**, *1*, 26.
- [59] E. Alinat, N. Delaunay, X. Archer, J.-M. Mallet, P. Gareil, *J. Hazard. Mater.* **2015**, *286*, 92. <https://doi.org/10.1016/j.jhazmat.2014.12.032>.
- [60] L. Huwei, F. Ruonong, *J. Anal. Appl. Pyrol.* **1988**, *14*, 163. [https://doi.org/10.1016/0165-2370\(88\)85006-X](https://doi.org/10.1016/0165-2370(88)85006-X).
- [61] S. C. Moldoveanu, *Analytical Pyrolysis of Natural Organic Polymers*, Vol. 1, Elsevier, Amsterdam **1998**.
- [62] J. A. Reilly, *JAIC Volume* **1991**, *30*, 145.
- [63] A. Quye, D. Littlejohn, R. A. Pethrick, R. A. Stewart, *Polym. Degrad. Stab.* **2011**, *96*(10), 1934. <https://doi.org/10.1016/j.polymdegradstab.2011.06.008>.
- [64] B. Kemper, D. A. Lichtblau, *Polym. Test.* **2019**, *80*, 106096. <https://doi.org/10.1016/j.polymertesting.2019.106096>.
- [65] P.-O. Bussiere, J.-L. Gardette, S. Therias, *Polym. Degrad. Stab.* **2014**, *107*, 246. <https://doi.org/10.1016/j.polymdegradstab.2014.02.022>.

SUPPORTING INFORMATION

Additional supporting information may be found online in the Supporting Information section at the end of this article.

How to cite this article: Elsässer C, Micheluz A, Pamplona M, Kavda S, Montag P. Selection of thermal, spectroscopic, spectrometric, and chromatographic methods for characterizing historical celluloid. *J Appl Polym Sci.* 2021;138: e50477. <https://doi.org/10.1002/app.50477>